Theoretical Investigation of Nitration and Nitrosation of Dimethylamine by N_2O_4

Chun Lin Lv, Yong Dong Liu,* and Rugang Zhong

College of Life Science & Bioengineering, Beijing University of Technology, Beijing 100124, P. R. China

Received: April 7, 2008; Revised Manuscript Received: May 22, 2008

Reactive nitrogen oxygen species (RNOS) contribute to the deleterious effects attributed to reacting with biomolecules. The mechanisms of the nitration and nitrosation of dimethylamine (DMA), which is the simplest secondary amine by N_2O_4, a member of RNOS, have been investigated at the CBS-QB3 level of theory. The nitration and nitrosation proceed via different pathways. The nitration of DMA follows three pathways. The first is the abstraction of the hydrogen atom of the amino group of DMA by the NO_2 radical followed by a recombination reaction of the resulting aminyl radical with another NO_2 radical. The second is DMA directly reacting with symmetrical O_2NNO_2 leading to dimethylnitramine via a concerted and a stepwise mechanism. The third is the reaction of DMA with asymmetrical $ONONO_2$. By computation, the main pathway for the formation of dimethylnitramine in the gas phase is by DMA directly reacting with asymmetrical $ONONO_2$. As to the nitrosation, a concerted mechanism for the reaction of DMA with asymmetrical $ONONO_2$ plays a major role in nitrosodimethylamine (NDMA) formation. In addition, the solvent effect on these nitration and nitrosation reactions has been also studied by using the implicit polarizable continuum model. Two major pathways of the formation of dimethylnitramine in water were found, and they are the radical process involving NO_2 and the concerted mechanism starting from symmetrical O_2NNO_2. The result of the nitrosation of DMA in water is consistent with that in the gas phase. Comparison of the energy barriers of each mechanism leads to the conclusion that the nitrosation is more favorable than the nitration in the reaction of DMA with N_2O_4. This conclusion is in good agreement with the experimental results. The results obtained here will help elucidate the mechanism of the lesions of biomolecules by RNOS.

1. Introduction

Previous studies have demonstrated that reactive nitrogen oxygen species (RNOS), believed to be N_2O_4 together with dinitrogen trioxide (N_2O_3), peroxynitrite ($ONOO^-$) and other nitric oxides,[1,2] are responsible for the causes of neurodegenerative and cardiovascular diseases as well as cancer.[3–11] Therefore, a great deal of research has been focused on the chemical property of RNOS and their reactions.[12–30] As a class of strong bioactivity intermediates, RNOS were found to react with a large number of biomolecules, including nucleic acids, lipids, and proteins, the results of which alter their structures and functions.[12–19] In order to better understand their bioactivity, the reactions of amines, existing in many biomolecules, with various RNOS have been extensively investigated, and the formation of nitrosamines and nitramines has been observed.[20–24]

In particular, the lesions of DNA and proteins by ONOOH and its conjugate base $ONOO^-$ have long been of interest.[25–30] However, the mechanisms by which the lesions are formed are not fully understood. Some experimental research has proposed that the nitration and nitrosation of biomolecules by ONOOH ($ONOO^-$) proceed via an indirect mechanism involving N_2O_4.[22,30]

In addition, N_2O_4 extensively exists in our environment and biological system. N_2O_4 is generally formed from the rapid dimerization of NO_2 (eq 3) and can be found in air and in water.[31,32] In vivo, N_2O_4 is endogenously formed by excess production of $NO^\bullet$ reacting with oxygen (eqs 1 and 3)[33,34] and by the decomposition of peroxynitrous acid (HOONO) (eqs 2 and 3).[35,36]

$$2\,{}^\bullet NO + O_2 \xrightarrow{k_1} 2NO_2^\bullet$$

$$\text{where } k_1 = 2.9\times10^6\ M^{-2}\ s^{-1} \tag{1}$$

$$HOONO \underset{k_{-2}}{\overset{k_2}{\rightleftharpoons}} {}^\bullet OH + NO_2^\bullet$$

$$\text{where } k_2 = 486\ s^{-1} \text{ and } k_{-2} = 2.4\times10^{10}\ M^{-1}\ s^{-1} \tag{2}$$

$$2NO_2^\bullet \underset{k_{-3}}{\overset{k_3}{\rightleftharpoons}} N_2 + O_4$$

$$\text{where } k_3 = 9\times10^8\ M^{-1}\ s^{-1} \text{ and } k_{-3} = 1.38\times10^4\ s^{-1} \tag{3}$$

In general, N_2O_4 has two isomeric forms:[31,37–41]

$$O_2NNO_2 \rightleftharpoons ONONO_2 \tag{4}$$

In view of the importance of N_2O_4 in the environment and in biology, further investigation is required to elucidate the mechanisms of the nitration and nitrosation by N_2O_4. White and his co-worker believed that the reaction of amines with symmetrical O_2NNO_2 and asymmetrical ON-ONO_2 proceeding via a nucleophilic displacement leads to nitramines and nitrosamines, respectively.[42] Later, Challis et al. pointed out that in the reaction of N-methylaniline in solution with gaseous NO_2, N-nitrosation derives from a dimer of asymmetrical ON-ONO_2, whereas N-nitration proceeds via a free-radical process involving NO_2.[24] Roncone et al. proposed that the reaction of tryptophan with N_2O_4 can lead to the formation of the major product of N-nitrosotryptophan.[43] Zhao et al. proposed a novel radical mechanism, and Lv et al. reported a concerted mechanism in the theoretical investigation of N-nitrosation of amines by N_2O_3.[44,45] In light of these previous studies, the authors of this paper proposed that different pathways account for the N-

* Corresponding author. Fax: +86-10-6739-2001. E-mail: ydliu@bjut.edu.cn.

10.1021/jp8029924 CCC: $40.75
Published on Web 07/10/2008

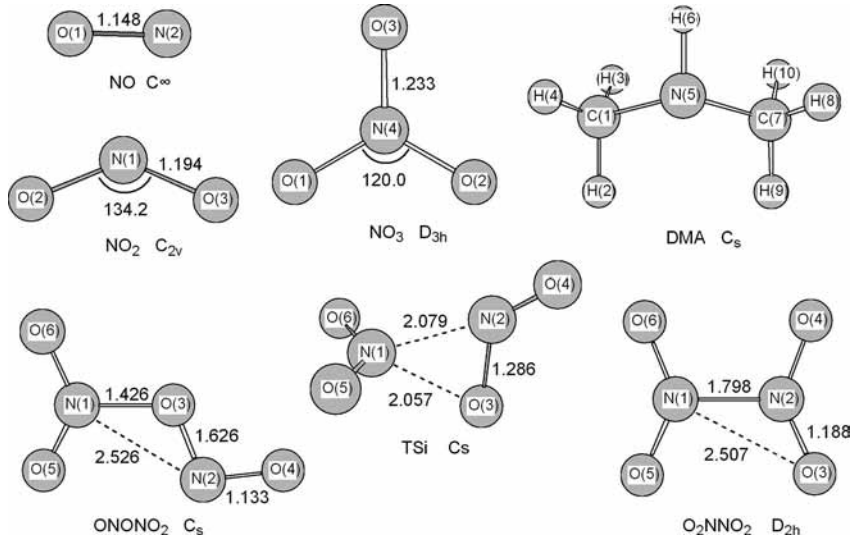

Figure 1. Geometries and main parameters of each species in the isomerization of N_2O_4 (distances in Angstroms).

nitration and the N-nitrosation of amines and that radical and nonradical mechanisms are involved in N_2O_4 reacting with amines.

To examine this proposal, a theoretical exploration of the mechanisms of N-nitration and N-nitrosation by N_2O_4 was carried out, and that exploration is reported in this paper. Dimethylamine (DMA), the simplest dialkylamine, was selected as the model subject.

2. Theoretical Methods

All the structures of reactants, transition states, intermediates, and products were fully optimized by using the hybrid density functional theory (DFT) by employing the B3LYP method (Becke's three-parameter nonlocal exchange functional[46] with the correlation functional of Lee, Yang, and Parr[47]), in conjunction with the 6-31G(d) basis set. Vibrational frequencies were also calculated at the same level of theory to characterize the nature of each stationary point. The minimum-energy path was obtained by using intrinsic reaction coordinate (IRC)[48] calculations to confirm the connection of each transition state with the designated equilibrium species. Reoptimizations of these stationary points were performed with the complete basis set (CBS-QB3) methodology, in which B3LYP density functional theory is combined with the 6-311G(2d,d,p) basis set (also denoted as the CBSB7 basis set).[49] All the calculations presented here were carried out with the GAUSSIAN-03 program package.[50]

The solvent effects of water, dimethyl sulfoxide (DMSO), and octanol on the reaction of DMA with N_2O_4 were also studied. On the basis of the optimized geometries at the B3LYP/CBSB7 level, the single-point energy calculation was performed with B3LYP and coupled cluster approximation by using single and double substitutions (CCSD)[51] at the 6-311G(d,p) level, by using the polarizable continuum podel (PCM),[52] denoted as PCM- B3LYP/6-311G(d,p)//B3LYP/CBSB7 and CCSD/6-311G(d,p)//B3LYP/CBSB7. The default dielectric constant (ε) of octanol was defined as 10.3,[53] and those of water and DMSO were taken from the GAUSSIAN-03 program.

3. Results and Discussion

The optimized structures of O_2NNO_2 and $ONONO_2$ and their corresponding transition state of isomerization (TSi) as well as the radicals produced from the decomposition of N_2O_4 are shown in Figure 1, and their calculated energies are listed in Table 1. The energy profile of isomerization of N_2O_4 is shown in Figure 2.

TABLE 1: Relative Energies (RE), Relative Enthalpy (RH), and Relative Gibbs Free Energies (RG) in the Gas Phase and Relative Energies in water (RE_w), in kcal/mol, as well as the Lowest Harmonic Vibrational Frequencies (LHVF), in cm^{-1} of each Equilibrium Species in the System of N_2O_4 Calculated at the CBS-QB3 Level

species	RE	RE_w[a]	RG	RH	LHVF
O_2NNO_2	0.00	0.00	0.00	0.00	94.2
TSi	44.45	49.19	44.54	44.45	640.8i
$ONONO_2$	7.23	2.99	5.90	7.23	34.8
$NO_2 + NO_2$	12.83	9.11	1.57	13.42	
$NO_3 + NO$	35.59	34.88	25.14	36.18	

[a] Calculated at PCM-CCSD/6-311G(d,p)//B3LYP/CBSB7.

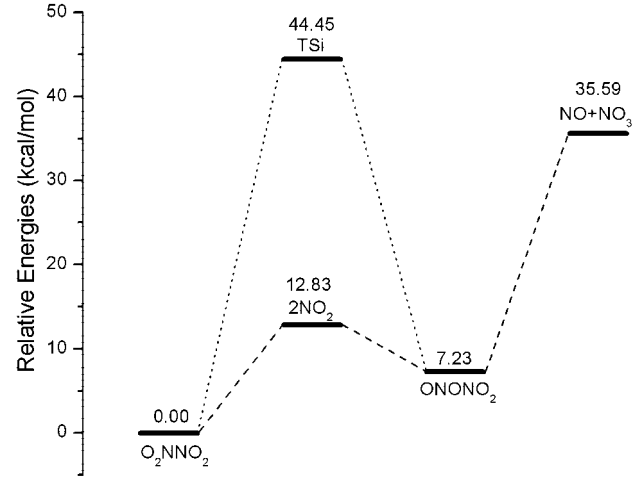

Figure 2. Schematic profiles of the potential energy surfaces of isomerization of N_2O_4 in the gas phase.

The Gibbs free energies for the dissociation of symmetrical O_2NNO_2 and asymmetrical $ONONO_2$ into two NO_2 radicals in the vacuum at 298 K were calculated as 1.57 and −4.33 kcal/mol, respectively and are in good agreement with the values from Ornellas[54] and Pimentel[55] (1.1 and −10.5 kcal/mol, respectively). In addition, the Gibbs free energy barrier for isomerization of symmetrical O_2NNO_2 into asymmetrical $ONONO_2$ was calculated to be 44.54 kcal/mol, whereas Pimentel

TABLE 2: Relative Energies (RE), Relative Enthalpy (RH), and Relative Gibbs Free Energies (RG) in the Gas Phase and Relative Energies in water (RE_w), in kcal/mol, as well as Lowest Harmonic Vibrational Frequencies (LHVF), in cm^{-1}, of each Stationary Point in the Reaction of DMA with $NO_2 + NO_2$ Calculated at the CBS-QB3 Level

species	RE	RE_w[a]	RG	RH	LHVF
DMA + NO_2	0.00	0.00	0.00	0.00	
CR1	−1.19	−1.98	3.10	−1.78	21.0
TS1	11.30	7.25	19.91	10.71	1329.7i
IM1	7.39	1.56	14.03	6.80	28.4
CP1	−36.57	−40.82	−16.26	−37.75	30.9
CR2	−1.42	−1.26	5.49	−2.01	14.1
TS2	17.36	8.87	25.24	16.77	1732.8i
IM2	6.73	0.59	12.80	6.14	27.2
CP2	−36.75	−41.45	−16.92	−37.93	30.6

[a] Calculated at PCM-CCSD/6-311G(d,p)//B3LYP/CBSB7.

TABLE 3: Relative Energies (RE), Relative Enthalpy (RH), and Relative Gibbs Free Energies (RG) in the Gas Phase and Relative Energies in water (RE_w), in kcal/mol, as well as Lowest Harmonic Vibrational Frequencies (LHVF), in cm^{-1}, of each Stationary Point in the Reaction of DMA with Symmetrical O_2NNO_2 Calculated at the CBS-QB3 Level

species	RE	RE_w[a]	RG	RH	LHVF
CR3	0.00	0.00	0.00	0.00	25.9
TS3	18.88	13.48	20.98	18.88	317.1i
CP3	−16.43	−25.63	−17.07	−16.44	28.5
TS4	41.12	51.85	43.29	40.74	1647.1i
IM3	18.43	19.99	21	18.06	48.8
TS5	23.86	25.26	26.96	23.49	137.8i
CP4	−17.53	−28.02	−20.13	−17.9	15.3
TS6	52.21	60.94	54.95	51.84	545.9i
CP5	−18.50	−27.12	−19.54	−18.87	16.8

[a] Calculated at PCM-CCSD/6-311G(d,p)//B3LYP/CBSB7.

TABLE 4: Relative Energies (RE), Relative Enthalpy (RH), and Relative Gibbs Free Energies (RG) in the Gas Phase and Relative Energies in water (RE_w), in kcal/mol, as well as Lowest Harmonic Vibrational Frequencies (LHVF), in cm^{-1}, of each Stationary Point in the Reaction of DMA with Asymmetrical $ONONO_2$ Calculated at the CBS-QB3 Level

species	RE	RE_w[a]	RG	RH	LHVF
DMA + $ONONO_2$	0.00	0.00	0.00	0.00	
CR4	−1.73	3.59	7.63	−2.32	21.9
TS7	5.73	22.33	16.44	5.14	101.8i
CP6	−31.00	−28.14	−20.61	−31.60	30.7
CR5	−10.46	−11.20	0.59	−11.06	27.8
TS8	−15.93	−15.09	−3.81	−16.52	294.9i
CP7	−28.99	−25.43	−18.61	−29.58	29.3

[a] Calculated at PCM-CCSD/6-311G(d,p)//B3LYP/CBSB7.

et al.[31] predicted that the energy barrier is 31.3 kcal/mol in the gas phase by using the DFT/B3LYP/13s8p(2d,1f) method.

It is well-known that NO_2 can rapidly dimerize to N_2O_4. However, NO_2 still coexists with N_2O_4 in the system[56] even though the concentration is relatively low. Thus, the nitrations of DMA by $NO_2 + NO_2$, symmetrical O_2NNO_2, and asymmetrical $ONONO_2$ will be discussed in the Sections 3.1, 3.2, and 3.3, respectively, and the nitrosation of DMA by N_2O_4 will be discussed in Section 3.4.

Considering the importance of entropy in these fragmental reactions, the relative Gibbs free energies (RG) in the gas phase are also shown in Tables 2–4. Obviously, the values of relative Gibbs free energies in the gas phase are in accordance with those of relative energies (RE). Moreover, no thermodynamic data in the solvent were obtained from the single-point energy calculations by using the implicit PCM model. Thus, unless otherwise noted, all energies discussed in the following parts are the calculated relative energies (RE).

3.1. Nitration of DMA by $NO_2 + NO_2$. Similarly to the nitrosation of DMA by $NO_2 + NO$,[44] the nitration of DMA by $NO_2 + NO_2$ begins with one NO_2 radical abstracting the hydrogen atom of the amino group of the DMA, leading to the formation of an aminyl radical. In a previous study, a transition state, in which the shifting hydrogen is syn to the nitroso group of O−NO, has been reported,[44] and its geometry is the same as that of TS1 optimized here (see Figure 3). Another transition state TS2 involving the formation of an anti-HONO moiety was also found and is shown in Figure 3. As can be seen from Figure 3, the partially forming O2−H4 bond lengths were calculated as 1.215 and 1.270 Å, in TS1 and TS2, respectively, whereas the partially breaking N5−H4 bond lengths were found to be 1.274 and 1.212 Å. The shifting hydrogen atom is closer to the oxygen atom in TS1 but is farther away from the oxygen atom in TS2, which suggests that the NO_2 in TS1 has a stronger ability to abstract the hydrogen from the amino group than that in TS2. Thus, the energy barrier at TS1 was calculated as 12.49 kcal/mol, lower than that at TS2 by about 6 kcal/mol (see Table 2). A lower energy barrier leads to the conclusion that DMA reacting with NO_2 predominantly proceeds via a syn-structure transition state (TS1).

Subsequently, the nascent aminyl radical in complexes of IM1 and IM2 was scavenged by another NO_2 radical without an energy barrier, resulting in dimethylnitramine formation, and the electronic rearrangements taking place have been detailed.[44]

Table 2 and Figure 4, demonstrate that the changes in enthalpies were found to be approximately 8 and −35 kcal/mol for the hydrogen transfer and nitration reaction, respectively. These enthalpy-change values indicate that although the intermediates formation is an endothermic reaction, the whole nitration of DMA is an exothermic process. Therefore, the nitration of DMA is a thermochemically favorable process.

3.2. Nitration of DMA with Symmetrical O_2NNO_2. The reaction of DMA with symmetrical O_2NNO_2 starts from a reactant complex CR3 which was formed by van de Waal's force, shown in Figure 5. The distances of N1−N15 and N1−N12 in CR3 were almost the same, calculated to be 2.825 and 2.809 Å, respectively. The close distance suggests that the nitrogen (N1) of DMA can perform a nucleophilic attack either on N15, proceeding via a concerted mechanism or N12, proceeding via a stepwise mechanism, to give rise to dimethylnitramine, as shown in Scheme 1 and as discussed in detail in the following sections.

3.2.1. Concerted Mechanism. The transition state of the nitration of DMA by symmetrical O_2NNO_2 by a concerted mechanism was found as TS3, in which the five atoms N1−H2−O11−N12−N15 compose a planar five-membered ring, shown in Figure 5. In TS3, the N1−H2 and N12−N15 bonds were elongated relative to their values in CR3 by 0.084 and 0.576 Å, respectively, whereas the distances of the forming N1−N15 and O11−H2 bonds were decreased to 1.806 and 1.477 Å, respectively. By starting from TS3, the IRC calculation along the backward reaction pathway clearly shows three types of geometric changes: one is the N−H bond decreasing, and the others are the NO_2 moieties of symmetrical O_2NNO_2 getting closer and complanation. These changes of structure in the reaction indicates that the derived energy of 18.89 kcal/mol at TS3 relative to CR3 is utilized to rotate the O_2N-NO_2 around the N−N bond, to dissociate the N−N bond, and to abstract

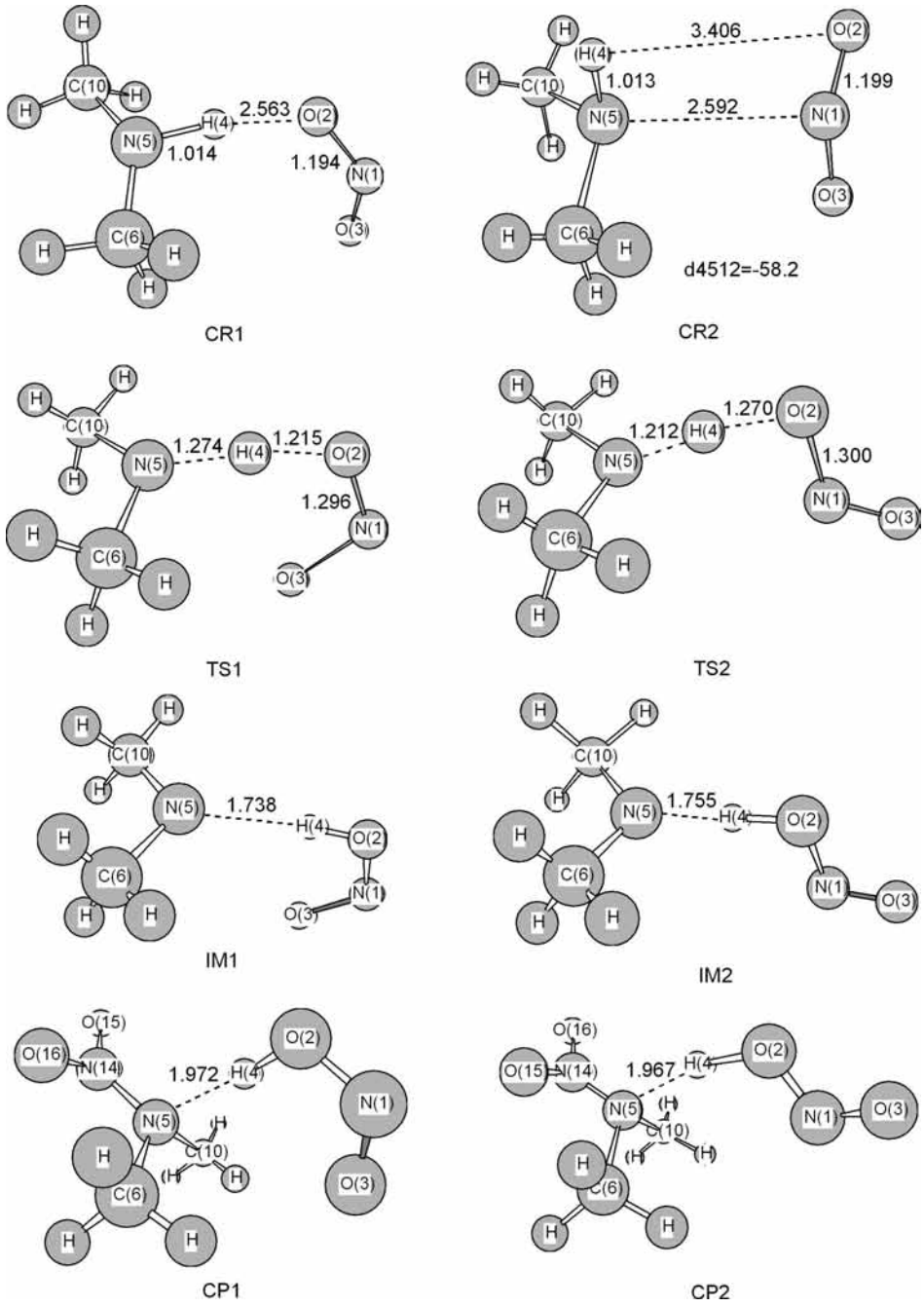

Figure 3. Geometries and main parameters of all the complexes and transition states involved in the reaction of DMA with $NO_2 + NO_2$ (distances in Angstroms).

the hydrogen from the amino group of DMA. Table 3 demonstrates that the Gibbs free energy of reaction for this nitration at the conditions of 298 K and 1 atm was calculated to be −17.07 kcal/mol. This negative value of Gibbs free energy change means that the reaction of DMA with symmetrical O_2NNO_2 can take place spontaneously.

3.2.2. Stepwise Mechanism. The stepwise mechanism of the nitration of DMA by symmetrical O_2NNO_2 involves two steps: the first is the addition of DMA to symmetrical O_2NNO_2, and the second is the hydrogen atom of the hydroxyl group transfers to the oxygen atom of the nitro moiety, resulting in dimethylnitramine formation.

Similarly to DMA adding to ONOH discussed by Lv and Liu,[45,57] the addition reaction of DMA with symmetrical O_2NNO_2, starting from the complex CR3, encountered a four-membered ring transition state TS4. The N1−H2 and N12−O11 bonds in TS4 were elongated from 1.015 and 1.189 Å in CR3 to 1.337 and 1.333 Å, respectively. These changes in bond length indicate that in TS4, the N1−H2 bond has been cloven, and the N12−O11 double bond has been changed to a partial double bond. The energy required for destroying these energetic bonds of N1−H2 and N12−O11 contributes to the high activation energy of DMA adding to symmetrical O_2NNO_2, calculated to be 41.12 kcal/mol in the gas phase. This addition reaction is completed with the generation of an intermediate IM3, where the N1−N12 (1.485 Å) and O11−H2 (0.974 Å) bonds have formed.

In the following reaction, the hydrogen transfers from the hydroxyl group to the oxygen of the NO_2 moiety. Notably, the hybridization of N12 in IM3 is more like sp^2, for there is a double bond between N12 and O13. On the basis of the molecular orbital theory, N12 prefers to bond with three (not

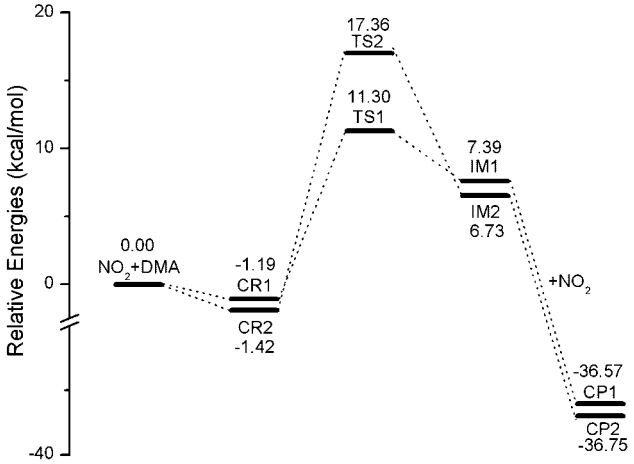

Figure 4. Schematic profiles of the potential energy surfaces of the reaction of DMA with $NO_2 + NO_2$ in the gas phase.

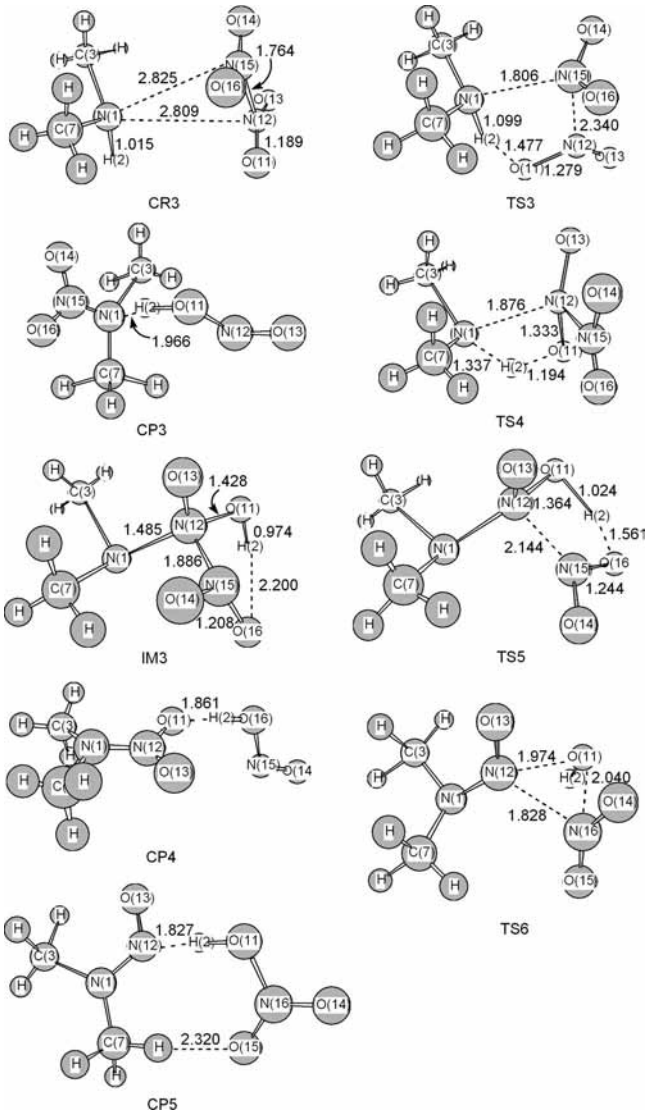

Figure 5. Geometries and main parameters of all the complexes, intermediates, and transition states involved in the reaction of DMA with symmetrical O_2NNO_2 (distances in Angstroms).

four) other atoms; thus, IM3 is unstable. With an activation energy of 5.43 kcal/mol, the departing group of the NO_2 moiety is able to abstract the hydrogen of the hydroxyl group and then leads to the formation of stable dimethylnitramine. Moreover,

SCHEME 1: Concerted and Stepwise Mechanistic Pathways of DMA Nitration

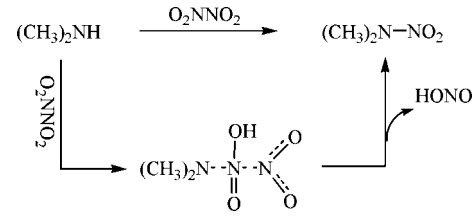

the 35.96 kcal/mol energy released in this hydrogen migration reaction supports this stabilization.

The profile shown in Figure 6 demonstrates the relative energy of each stationary point along the reaction pathway of DMA nitration by symmetrical O_2NNO_2. Proceeding via the stepwise mechanism, the addition reaction with a high activation energy of 41 kcal/mol is the rate-determining step of the reaction of DMA with symmetrical O_2NNO_2. Compared to the stepwise mechanism, the concerted mechanism has a lower energy barrier. As a result of the lower energy barrier, the authors conclude that the reaction of DMA with symmetrical O_2NNO_2 prefers the concerted mechanism.

3.3. Nitration of DMA with Asymmetrical $ONONO_2$. In the case of nitration of DMA by the asymmetrical $ONONO_2$, a complex CR4 was first formed. As shown in Figure 7, the N6−H7−O5−N1−O2−N3 in CR4 composed a six-membered ring. This structure facilitates the lone pair of electrons of the N6 to attack the N3 with a partial positive charge. Further changes of the structure encountered a transition state TS7, shown in Figure 7. In TS7, the broken N3−O2 bond was elongated from 1.358 in CR4 to 1.835 Å, whereas the forming N3−N6 bond length was decreased from 3.542 to 2.481 Å, but the N6−H7 bond length did not change. These structural changes, for which the N3 binding to N6 is prior to the departure of nitrous acid (HONO), are consistent with the characteristic of the addition−elimination reaction. The energy needed to reach the transition state TS7 was calculated to be 7.46 kcal/mol.

Scheme 2 shows the movement of electrons in the nitration of DMA by asymmetrical $ONONO_2$. This nitration process is driven by the lone pair of electrons of the N6 attacking the nitrogen of the NO_3 moiety of $ONONO_2$. Nitrogen can accommodate only eight electrons in its valence shell; threfore, the N3−O2 bond must begin to break as the N6−N3 bond begins to form, as can be seen from the electronic structure of TS7. Also, the movements of electrons lead to the oxygen atom of

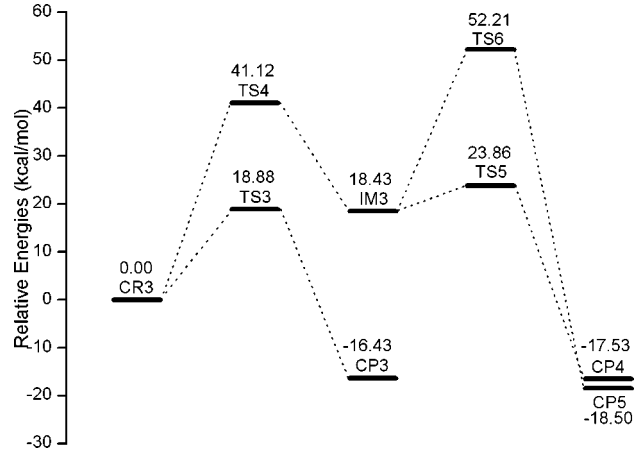

Figure 6. Schematic profiles of the potential energy surfaces of the reaction of DMA with symmetrical O_2NNO_2 in the gas phase.

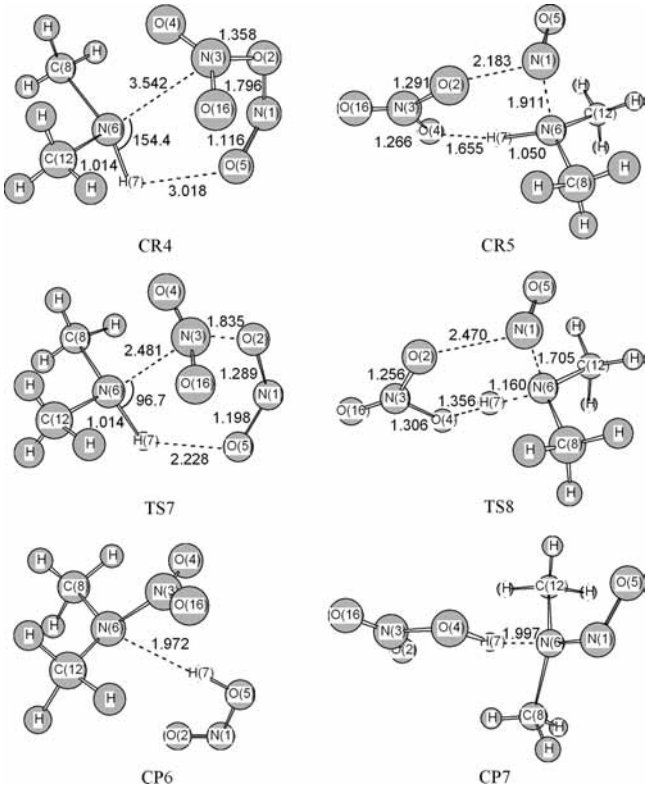

Figure 7. Geometries and main parameters of all the complexes and transition states involved in the reaction of DMA with asymmetrical $ONONO_2$ (distances in Angstroms).

the NO moiety with more negative charge and to the hydrogen atom with more positive charge. The final result of the movement of electrons is to facilitate the departure of HONO.

3.4. Nitrosation of DMA. The nitrosation of DMA by N_2O_4 can proceed via three possible mechanistic pathways (see Scheme 3).

As shown in Figure 2, the energy required for the decomposition of asymmetrical $ONONO_2$ to NO + NO_3 was calculated to be 35.59 kcal/mol, which is higher than that for the decomposition to two NO_2 radicals. This means that no product of NO + NO_3 forms, and no further reaction can take place; therefore, the pathway 1 (p1) has no contribution to the nitrosation of DMA. Regarding p2, the high energy barrier (41.12 kcal/mol, shown in Figure 6) for the addition of DMA to O_2NNO_2 indicates that the reaction of DMA with O_2NNO_2 proceeds preferentially via the concerted mechanism; thus, p2 is not the main pathway for DMA nitrosation. Pathway 3 (p3), proceeding via a concerted mechanism, will be discussed in the following section.

The reaction of DMA with asymmetrical $ONONO_2$ starts from a complex CR5, shown in Figure 7. In CR5, the bond length of N1−O2 is 2.183 Å. This bond length indicates that with the energy released from the stabilization of intermolecular interaction, the N1−O2 bond has been broken. Subsequently, the reaction of DMA with asymmetrical $ONONO_2$ encountered a transition state TS8, in which N1−N6−H7−O4−N3−O2 composes a planar six-membered ring, shown in Figure 7. TS8 has only one imaginary frequency of 294.9i cm^{-1}, corresponding to the hydrogen and NO moiety vibration. Further IRC calculation showed that TS8 connected the reactant complex CR5 and the product complex CP7 (see Figure 8 in the Supporting Information). In TS8, the N6−H7 bond length was elongated to 1.160 Å, whereas the N1−N6 and O4−H7 bond lengths were decreased to 1.705 and 1.356 Å, respectively. These changes in bond length indicate that the hydrogen atom transfer from N6 to O4 is driven by the coaction of the push effect of the nitroso group and the abstracting effect of the oxygen of the nitro group (Scheme 4).

For this coaction, the nitrosation of DMA by asymmetrical $ONONO_2$ is barrierless. As can be seen from Figure 8 in the Supporting Information, the potential energy surface (PES) between TS8 and CR5 is very flat. The energy relative to the reactant complex CR5 at TS8 was calculated to be 0.73 kcal/mol at the B3LYP/CBSB7 level. However, with zero-point vibrational energy corrections, the energy barrier was found to be −1.17 kcal/mol at B3LYP/CBSB7 and −5.46 kcal/mol by the CBS-QB3 method.

3.5. Effects of Solvent. It is well-known that biotransformation reactions take place in an emulsion of fat/water in vivo. As a model, the octanol/water mixture was selected to simulate the fat/water medium in early studies.[58–60] In this paper, octanol ($\varepsilon = 10.3$), water ($\varepsilon = 78.4$), and DMSO ($\varepsilon = 46.7$), the default dielectric constant of which is in the middle between octanol and water, were selected to investigate the solvent effect on the nitration and nitrosation reactions by using the PCM-B3LYP/6-311+G(d,p)//B3LYP/CBSB7 method. By computation, the relative energies of each stationary point in water, DMSO, and octanol were found to be nearly identical (evidence for this finding can be found in the Supporting Information), indicating that the solvent effect on the nitration and nitrosation reactions is independent of the kind of solvent. Therefore, a higher method of PCM-CCSD/6-311G(d,p) was used to calculate the single-point energy of each structure in water. It is notable that the PCM as an implicit solvent model gives excellent results in treating the strong long-range solute−solvent interactions which dominate many solvation phenomena but poorly simulates the influence of the microconformation of real solution on the solvation of the solute molecules.

As can be seen from Table 1, in aqueous solvation, the energy required for the homolysis cleavage of the N1−N2 bond in O_2NNO_2 was decreased by 3.72 kcal/mol, whereas that of the N1−O3 bond in $ONONO_2$ was slightly increased by 0.5 kcal/mol, and the activation energy at TSi was increased by 4.74 kcal/mol, compared to the energy values in the gas phase; therefore, the intertransformation of O_2NNO_2 with $ONONO_2$ in aqueous solvation is still proceeding via the process of homolysis cleavage and radical recombination. The inclusion of the solvent effect in single-point energy calculation significantly decreased the energy barriers of the hydrogen abstracting reactions. The energy barriers at TS1 and TS2, which were calculated in the gas phase as 12.49 and 18.78 kcal/mol, respectively, became 9.23 and 10.13 kcal/mol, respectively, in water. In addition, the energy barrier of the nitration of DMA by symmetrical O_2NNO_2 was decreased from 18.88 kcal/mol in the gas phase to 13.48 kcal/mol in aqueous solvation for the concerted mechanism and increased by 10.73 kcal/mol for the stepwise mechanism. The water effect increased the energy barrier for the nitration of DMA by asymmetrical $ONONO_2$ by 11.28 kcal/mol. Otherwise stated, in water, the nitration of DMA may easily proceed via a radical process involving NO_2 and a concerted mechanism starting from symmetrical O_2NNO_2.

The relative energy at TS8 in aqueous solvation was slightly increased by 1.58 kcal/mol relative to that in the gas phase, the reason for this may be the solvation of the nitrogen of DMA in aqueous solvation. However, the negative value of the relative energy at TS8 indicated that once the asymmetrical $ONONO_2$ isomer forms, the nitrosation of DMA by asymmetrical $ONONO_2$ even in aqueous solvation is barrierless. The activation

SCHEME 2: Movements of Electrons in the Nitration of DMA by Asymmetrical $ONONO_2$

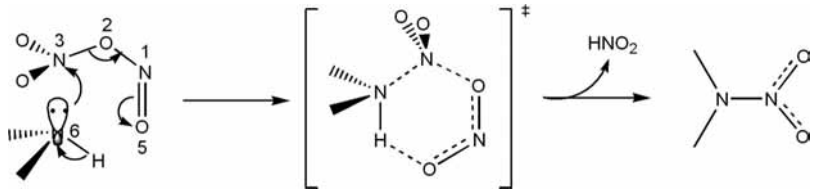

SCHEME 3: Potential Pathways for the Nitrosation of DMA by N_2O_4

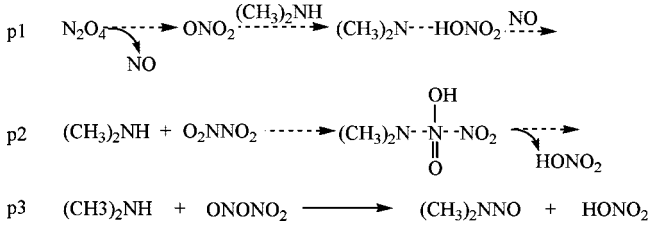

SCHEME 4: Movements of Electrons in the Nitrosation of DMA by Asymmetrical $ONONO_2$

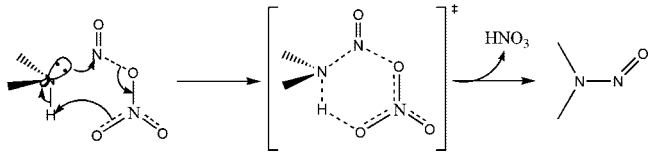

energy of nitrosation being lower than that of nitration is in good agreement with the experimental observation that more nitrosation than nitration is produced.[43]

4. Conclusion

The mechanisms of nitrosation and nitration of DMA by N_2O_4 have been investigated at the CBS-QB3 level of theory. It was found that nitration and nitrosation proceed via different pathways. Regarding the nitration of DMA, there are three pathways. The first is the NO_2 radical abstracting the hydrogen atom of the amino group of DMA followed by a recombination reaction of the resulting aminyl radical with another NO_2 radical. The second is DMA directly reacting with symmetrical O_2NNO_2 leading to dimethylnitramine via a concerted and a stepwise mechanism. The last is the reaction of DMA with asymmetrical $ONONO_2$. The computation shows that DMA directly reacting with asymmetrical $ONONO_2$ is the major pathway of dimethylnitramine formation in the gas phase, with a calculated energy barrier of 7.46 kcal/mol. However, other pathways which have low energy barriers also play a role in the formation of dimethylnitramine. As to the nitrosation of DMA, the radical mechanism involving NO_3 and NO and the stepwise mechanism in DMA reacting with symmetrical O_2NNO_2 resulting in NDMA formation are energy-demanding processes. The nitrosation of DMA by asymmetrical $ONONO_2$ was proved to contribute to NDMA formation.

The solvent effects of water, DMSO, and octanol on the nitration and nitrosation of DMA have been studied in this paper. The calculations were performed by using the implicit PCM model. It was found that after the inclusion of the solvent effect, the main pathway of nitration changes from DMA reacting directly with asymmetrical $ONONO_2$ to a radical process involving NO_2 and a concerted mechanism starting from symmetrical O_2NNO_2. The result of the nitrosation of DMA in water is consistent with that in the gas phase.

Comparison of the energy barriers of each mechanism reveals that nitrosation is more favorable than nitration in the reaction of DMA with N_2O_4. On the basis of the theoretical results obtained here, the observation that the production of nitrosation was more than that of nitration[43] can be explained, and some guide for exploring the mechanisms of nitration and nitrosation of secondary amines by other RNOS can be provided.

Acknowledgment. The authors thank Peter King. P. Eng. of Beijing University of Technology for English language suggestions. This work was supported by the National Natural Science Foundation of China (no. 20672011) and National Natural Science Foundation of Beijing (no. 8072006) and PHR (IHLB).

Supporting Information Available: Relative energies in different solvents, and reaction potential energy surface of the nitrosation of DMA by asymmetrical $ONONO_2$. This material is available free of charge via the Internet at http://pubs.acs.org.

References and Notes

(1) Grisham, M. B.; Jourd'Heuil, D.; Wink, D. A. *Am. J. Physiol.* **1999**, *39*, G315.
(2) Mak, A. M.; Wong, M. W. *Chem. Phys. Lett.* **2005**, *403*, 192.
(3) Beckman, J. S.; Koppenol, W. H. *Am. J. Physiol.* **1996**, *271*, C1424.
(4) Rubbo, H.; Darley-Usmar, V.; Freeman, B. A. *Chem. Res. Toxicol.* **1996**, *9*, 809.
(5) Stamler, J. S.; Singel, D. J.; Loscalzo, J. *Science* **1992**, *258*, 1898.
(6) Sawa, T.; Ohshima, H. *Nitric Oxide Biol. Chem.* **2006**, *14*, 91.
(7) Laval, F.; Wink, D. A. *Carcinogenesis* **1994**, *15*, 443.
(8) Wink, D. A.; Vodovotz, Y.; Laval, J.; Laval, F.; Dewhirst, M. W.; Mitchell, J. B. *Carcinogenesis* **1998**, *9*, 711.
(9) Cook, J. A.; Krishna, M. C.; Pacelli, R.; DeGraff, W.; Liebmann, J.; Russo, A.; Mitchell, J. B.; Wink, D. A. *Br. J. Cancer* **1997**, *76*, 325.
(10) Wink, D. A.; Cook, J. A.; Christodoulou, D.; Krishna, M. C.; Pacelli, R.; Kim, S.; DeGraff, W.; Gamson, J.; Vodovotz, Y.; Russo, A.; Mitchell, J. B. *Nitric Oxide Biol. Chem.* **1997**, *1*, 3.
(11) Dedon, P. C.; Tannenbaum, S. R. *Arch. Biochem. Biophys.* **2004**, *423*, 12.
(12) Suzuki, T.; Mower, H. F.; Friesen, M. D.; Gilibert, I.; Sawa, T.; Ohshima, H. *Free Radical Bio. Med.* **2004**, *37*, 671.
(13) Wink, D. A.; Kasprzak, K. S.; Maragos, C. M.; Elespuru, R. K.; Misra, M.; Dunams, T. M.; Cebula, T. A.; Koch, W. H.; Andrews, A. W.; Allen, J. S.; Keefer, L. K. *Science* **1991**, *254*, 1001.
(14) Burney, S.; Caulfield, J. L.; Niles, J. C.; Wishnok, J. S.; Tannenbaum, S. R. *Mutat. Res.* **1999**, *424*, 37.
(15) Szabo, C.; Ohshima, H. *Nitric Oxide Biol. Chem.* **1997**, *1*, 373.
(16) Wiseman, H.; Halliwell, B. *Biochem. J.* **1996**, *313*, 17.
(17) Davis, K. L.; Martin, E.; Turko, I. V.; Murad, F. *Annu. Rev. Pharmacol. Toxicol.* **2001**, *41*, 203.
(18) Ohshima, H.; Yermilov, V.; Yoshie, Y.; Rubio, J. *Advances in DNA Damage and Repair*; Plenum Publishers: New York, 1999; p 329.
(19) Masuda, M.; Nishino, H.; Ohshima, H. *Chem-Biol. Interact.* **2002**, *139*, 187.
(20) Blanchard, B.; Dendane, M.; Gallard, J. F.; Levin, C. H.; Karim, A.; Payen, D.; Launay, J. M.; Ducrocq, C. Oxidation. *Nitric Oxide Biol Chem.* **1997**, *1*, 442.
(21) Lakshmi, V. M.; Hsu, F. F.; Zenser, T. V. *Chem. Res. Toxicol.* **2002**, *15*, 1059.
(22) Masuda, M.; Mower, H. F.; Pignatelli, B.; Celan, I.; Friesen, M. D.; Nishino, H.; Ohshima, H. *Chem. Res. Toxicol.* **2000**, *13*, 301.
(23) Lakshmi, V. M.; Hsu, F. F.; Davis, B. B.; Zenser, T. V. *Chem. Res. Toxicol.* **2001**, *14*, 312.
(24) Challis, B. C.; Shuker, D. E.; Fine, D. H.; Goff, E. U.; Hoffman, G. A. *IARC Scientific Publication* **1982**, *41*, 11.

(25) Tsai, H. H.; Hamilton, T. P.; Tsai, J. H. M.; Woerd, M.; Harrison, J. G.; Jablonsky, M. J.; Beckman, J. S.; Koppenol, W. H. *J. Phys. Chem.* **1996**, *100*, 15087.
(26) Musaev, D. G.; Geletii, Y. V.; Hill, C. L. *J. Phys. Chem. A* **2003**, *107*, 5862.
(27) Satarug, S.; Haswell-Elkins, M. R.; Tsuda, M.; Mairiang, P.; Sithithaworn, P.; Mairiang, E.; Esumi, H.; Sukprasert, S.; Yongvanit, P.; Elkins, D. B. *Carcinogenesis* **1996**, *17*, 1075.
(28) Miranda, K. M.; Espey, M. G.; Yamada, K.; Krishna, M.; Ludwick, N.; Kim, S.; Jourd'heuili, D.; Grishami, M. B.; Feelischi, M.; Fukuto, J. M.; Wink, D. A. *J. Biol. Chem.* **2001**, *276*, 1720.
(29) Houk, K. N.; Condroski, K. R.; Pryor, W. A. *J. Am. Chem. Soc.* **1996**, *118*, 13002.
(30) Pryor, W. A.; Squadrito, G. L. *Am. J. Phys.* **1995**, *268*, L699.
(31) Pimentel, A. S.; Lima, F. C. A.; Silva, A. B. F. *J. Phys. Chem. A* **2007**, *111*, 2913.
(32) Choi, J.; Valentine, R. L. *Environ. Sci. Technol.* **2003**, *37*, 4871.
(33) Goldstein, S.; Czapski, G. *J. Am. Chem. Soc.* **1995**, *117*, 12078.
(34) Grätzel, M.; Henglein, A.; Lilie, J.; Beck, G. *Ber. Bunsen-Ges. Phys. Chem.* **1969**, *73*, 646.
(35) Richeson, C. E.; Mulder, P.; Bowry, V. W.; Ingold, K. U. *J. Am. Chem. Soc.* **1998**, *120*, 7211.
(36) Tsang, W.; Herron, J. T. *J. Phys. Chem. Ref. Data* **1991**, *20*, 609.
(37) Zhao, Y. L.; Houk, K. N.; Olson, L. P. *J. Phys. Chem. A* **2004**, *108*, 5864.
(38) Louis, R. V.; Kcrawford, B. *J. Chem. phys.* **1965**, *42*, 857.
(39) Forney, D.; Thompson, W. E.; Jacox, M. E. *J. Chem. Phys.* **1993**, *99*, 7393.
(40) Wang, J.; Voss, M. R.; Busse, H.; Koel, B. E. *J. Phys. Chem. B* **1998**, *102*, 4693.
(41) Wang, J.; Koel, B. E. *J. Phys. Chem. A* **1998**, *102*, 8573.
(42) White, E. H.; Feldman, W, R. *J. Am. Chem. Soc.* **1957**, *79*, 5832.
(43) Roncone, R.; Barbieri, M.; Monzani, E.; Casella, L. *Coordin. Chem. Rev.* **2006**, *250*, 1286.
(44) Zhao, Y. L.; Garrison, S. L.; Gonzalez, C.; Thweatt, W. D.; Marquez, M. *J. Phys. Chem. A* **2007**, *111*, 2200.
(45) Lv, C. L.; Liu, Y. D.; Wang, Y. H.; Zhong, R. G. *Acta Chim. Sin.* **2007**, *65*, 1568.
(46) Becke, A. D. *J. Chem. Phys.* **1993**, *98*, 5648.
(47) Lee, C. T.; Yang, W. T.; Parr, R. G. *Phys. Rev. B* **1988**, *37*, 785.
(48) Gonzalez, C.; Schlegel, H. B. *J. Chem. Phys.* **1989**, *90*, 2154.
(49) (a) Montgomery, J. A.; Frisch, M. J.; Ochterski, J. W.; Petersson, G. A. *J. Chem. Phys.* **1999**, *110*, 2822. (b) See Gaussian thermochemistry white papers and technical notes, http://www. gaussian.com/gwhitepap/thermo.htm.
(50) Frisch, M. J.; Trucks, G. W.; Schlegel, H. B.; Scuseria, G. E.; Robb, M. A.; Cheeseman, J. R.; Montgomery, J. A., Jr.; Vreven, T.; Kudin, K. N.; Burant, J. C.; Millam, J. M.; Iyengar, S. S.; Tomasi, J.; Barone, V.; Mennucci, B.; Cossi, M.; Scalmani, G.; Rega, N.; Petersson, G. A.; Nakatsuji, H.; Hada, M.; Ehara, M.; Toyota, K.; Fukuda, R.; Hasegawa, J.; Ishida, M.; Nakajima, T.; Honda, Y.; Kitao, O.; Nakai, H.; Klene, M.; Li, X.; Knox, J. E.; Hratchian, H. P.; Cross, J. B.; Bakken, V.; Adamo, C.; Jaramillo, J.; Gomperts, R.; Stratmann, R. E.; Yazyev, O.; Austin, A. J.; Cammi, R.; Pomelli, C.; Ochterski, J. W.; Ayala, P. Y.; Morokuma, K.; Voth, G. A.; Salvador, P.; Dannenberg, J. J.; Zakrzewski, V. G.; Dapprich, S.; Daniels, A. D.; Strain, M. C.; Farkas, O.; Malick, D. K.; Rabuck, A. D.; Raghavachari, K.; Foresman, J. B.; Ortiz, J. V.; Cui, Q.; Baboul, A. G.; Clifford, S.; Cioslowski, J.; Stefanov, B. B.; Liu, G.; Liashenko, A.; Piskorz, P.; Komaromi, I.; Martin, R. L.; Fox, D. J.; Keith, T.; Al-Laham, M. A.; Peng, C. Y.; Nanayakkara, A.; Challacombe, M.; Gill, P. M. W.; Johnson, B.; Chen, W.; Wong, M. W.; Gonzalez, C.; Pople, J. A. *Gaussian 03*, revision C.02; Gaussian, Inc.: Wallingford, CT, 2004.
(51) Scuseria, G. E.; Schaefer, H. F., III *J. Chem. Phys.* **1989**, *90*, 3700.
(52) Tomasi, J.; Persico, M. *Chem. Rev.* **1994**, *94*, 2027.
(53) Steel, W. H.; Walker, R. A. *Nature* **2003**, *424*, 296.
(54) Ornellas, F. R.; Resende, S. M.; Machado, F. B. C.; Roberto-Neto, O. *J. Chem. Phys.* **2003**, *118*, 4060.
(55) Pimentel, A. S.; Lima, F. C. A.; Silva, A. B. F. *Chem. Phys. Lett.* **2007**, *436*, 47.
(56) Kato, T. *J. Chem. Phys.* **2004**, *120*, 10127.
(57) Lv, C. L.; Liu, Y. D.; Zhong, R. G. *J. Mol. Struct. (THEOCHEM)* **2007**, *802*, 1.
(58) Eisfeld, W.; Maurer, G. *J. Phys. Chem. B* **1999**, *103*, 5716.
(59) Lamarche, O.; Platts, J. A.; Hersey, A. *J. Chem. Inf. Comput. Sci.* **2004**, *44*, 848.
(60) Lv, C. L.; Liu, Y. D.; Zhong, R. G. *Theor. Chem. Acc.* **2007**, *118*, 973.

JP8029924